Biomechanical Study of Pediatric Human Cervical Spine: A Finite Element Approach

Srirangam Kumaresan
Narayan Yoganandan[1]
Frank A. Pintar
Dennis J. Maiman
Department of Neurosurgery,
Medical College of Wisconsin and
Department of Veterans Affairs Medical Center,
Milwaukee, WI 53295

Shashi Kuppa
Conrad Technologies, Inc.,
Washington, DC 20202

Although considerable effort has been made to understand the biomechanical behavior of the adult cervical spine, relatively little information is available on the response of the pediatric cervical spine to external forces. Since significant anatomical differences exist between the adult and pediatric cervical spines, distinct biomechanical responses are expected. The present study quantified the biomechanical responses of human pediatric spines by incorporating their unique developmental anatomical features. One-, three-, and six-year-old cervical spines were simulated using the finite element modeling technique, and their responses computed and compared with the adult spine response. The effects of pure overall structural scaling of the adult spine, local component developmental anatomy variations that occur to the actual pediatric spines, and structural scaling combined with local component anatomy variations on the responses of the pediatric spines were studied. Age- and component-related developmental anatomical features included variations in the ossification centers, cartilages, growth plates, vertebral centrum, facet joints, and annular fibers and nucleus pulposus of the intervertebral discs. The flexibility responses of the models were determined under pure compression, pure flexion, pure extension, and varying degrees of combined compression–flexion and compression–extension. The pediatric spine responses obtained with the pure overall (only geometric) scaling of the adult spine indicated that the flexibilities consistently increase in a uniform manner from six- to one-year-old spines under all loading cases. In contrast, incorporation of local anatomic changes specific to the pediatric spines of the three age groups (maintaining the same adult size) not only resulted in considerable increases in flexibilities, but the responses also varied as a function of the age of the pediatric spine and type of external loading. When the geometric scaling effects were added to these spines, the increases in flexibilities were slightly higher; however, the pattern of the responses remained the same as found in the previous approach. These results indicate that inclusion of developmental anatomical changes characteristic of the pediatric spines has more of a predominant effect on biomechanical responses than extrapolating responses of the adult spine based on pure overall geometric scaling. [S0148-0731(00)00501-X]

Introduction

It is common anatomical knowledge that the pediatric cervical spine is not a scaled-down version of the adult human [1]. Growth and developmental processes occur throughout the first two decades of human life to attain skeletal maturity [2–5]. For example, ossification centers gradually coalesce to form the vertebrae devoid of the cartilage centers that include, for the typical cervical vertebra, the neurocentral, spinous, and transverse processes cartilages [6,7]. Similarly, the nucleus and annulus of the intervertebral discs change [8,9]. The orientation of the facet joints changes during the early part of human cervical spine development [10]. These distinct structural and anatomic variations are especially noteworthy in the one-, three-, and six-year age groups of the pediatric population. These are discussed below [11].

During the fetal stage, the membranous structure of the vertebrae develops and subsequently ossifies at birth [11,7]. The ossification process is a bony formation from the cartilaginous structure, which continues from birth to adulthood to achieve skeletal maturity (Fig. 1). The one-year-old cervical vertebra is comprised of three ossification centers connected by the soft cartilage. Throughout early childhood, fusion of ossification centers occurs. At three years of age, the ossification centers of the vertebrae fuse posteriorly, and anterior fusion occurs by six years of age. The

facet joint anatomy also unergoes changes in these vertebrae as a function of age (Fig. 2). Compared to the adult, pediatric vertebrae lack the secondary ossification uncinate processes. Pediatric vertebrae are connected to the intervertebral discs through the medium of growth plates. In addition to the unique variations in vertebrae anatomy, notable developmental changes occur to the intervertebral disc. Pediatric discs are characterized by a relatively larger size nucleus with a lack of clear demarcation between the loosely embedded fibers in the ground substance and nucleus pulposus (Fig. 3). During maturation, the fibers in the ground substance stiffen and distinguish the annulus from the nucleus [8]. These structural features indicate that the pediatric spine not only differs consierably from the adult, but also varies among the different ages of the pediatric population.

Because of the important differences in the above-cited three age groups, and because no published studies systematically analyze and evaluate the differences in the biomechanical properties of these cervical spines as a function of external loading, mathematical modeling research was adopted in this study. Specifically, finite element models of the three pediatric cervical spines were developed by incorporating their unique anatomical characteristics. The biomechanical responses in terms of overall flexibility of the models were compared with the skeletally mature adult spine under the following loading modes: pure compression, pure flexion, pure extension, and varying degrees of combined compression–flexion and compression–extension. The effects of pure overall structural scaling (method adopted to obtain the pediatric response from the adult spine), local component geometric
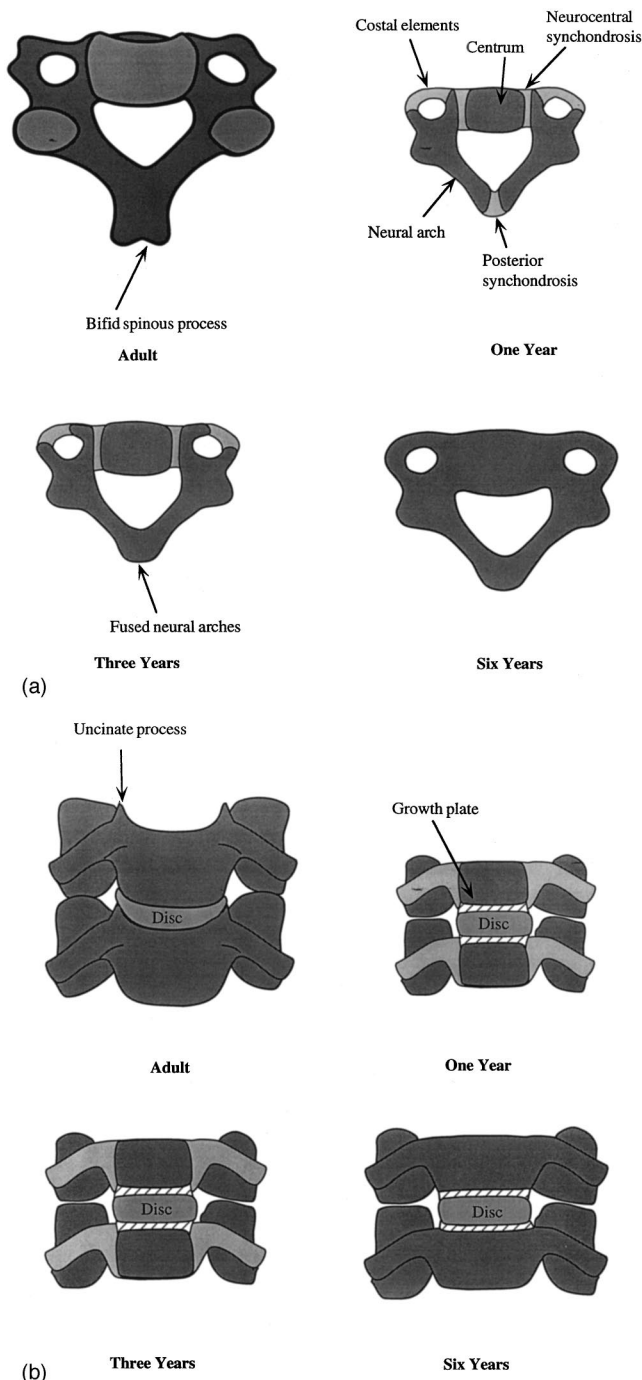
Fig. 1   (*a*) Schematic of the one-, three-, and six-year-old, and adult human cervical spine vertebra (superior view). In the one-year-old vertebra, the ossification centers (centrum and neural arches) are loosely connected by cartilage materials (synchondroses). In the three-year-old vertebra, the neural arches fuse with each other posteriorly. In the six-year-old vertebra, the neural arches fuse with vertebral centrum anteriorly. In adult vertebra, primary ossification centers (centrum and neural arches) fuse completely and secondary ossification centers (uncinates and bifid spinous process) fuse with primary ossification centers. (*b*) Schematic of the one-, three-, and six-year-old, and adult human cervical spine functional spinal unit (anterior view). In the one-, three-, and six-year-old, the superior and inferior growth plates, and the flat vertebral centrum without uncinates are seen. In the adult vertebra, saddle-shaped uncinates are seen.

and material properties variations, and structural scaling combined with local component geometric and material properties variations, were investigated in the present study (Fig. 4).

Methods

The one-, three-, and six-year-old cervical spine (C4–C5–C6) finite element models were developed by systematically modifying the anatomically accurate and experimentally validated adult model. A detailed description of the development and validation of the adult model is presented in previous publications [12–15]. For the sake of completeness, details of the adult model are presented. The geometric details for the C4, C5, and C6 vertebrae of the adult model were obtained from the sagittal and coronal computed tomography images from a 33-year-old human cadaver free from spinal disease or trauma. The images were processed using an edge detection algorithm to extract the outlines of the vertebral sections and the processed images were sequentially stacked to define a three-dimensional wire mesh. Surfaces were created by defining a series of four closed-loop boundary curves for the wire meshes and solids were formed by filling the volume defined by a group of six surfaces. This methodology resulted in a solid model of the C4, C5, and C6 vertebrae. The bony regions of the vertebrae included the cortical bone, cancellous bone, endplates, laminae, pedicles, lateral masses, transverse processes, and spinous processes. The soft tissue structures, i.e., intervertebral discs, facet joints (articular cartilage, synovial fluid, and synovial membrane along with capsular ligament), uncovertebral joints, and all ligaments (anterior and posterior longitudinal ligament, ligamentum flavum, and interspinous ligament) were added to the model using the cryomicrotome anatomy images. The cancellous bone, cortical bone, endplates, and posterior elements of the three vertebrae, and articular cartilages in the facet joints were modeled using isoparametric eight-noded solid elements. The annulus fibrosus of the intervertebral disc were defined using the fiber-reinforced concrete approach: The collagen fibers were modeled using tension-active rebar elements and the ground substance matrix was defined using solid elements. The fiber content was set at 20 percent of the annulus volume and arranged in an alternating criss-cross manner with 25 deg orientation [16,17]. The fluid constituents of the spine in the nucleus pulposus of the intervertebral disc, and in the uncovertebral and facet joints, were modeled using three-dimensional fluid elements [13]. These element idealizations incorporate the incompressible nature of the fluid medium. Previous studies have indicated that the fluid constituents are incompressible [18,19]. The choice of fluid elements (Poisson's ratio of 0.5) better simulates the material behavior of fluid constituents (incompressibility) compared to solid elements with a Poisson's ratio of 0.49 (closer to 0.5). A similar approach has been used in previous finite element spine modeling studies [20,21]. The synovial membranes enclosing the uncovertebral and facet joints were modeled using three-dimensional membrane elements. All ligaments were modeled using nonlinear tension-active cable elements. The adult model included 12,712 elements with 15,577 nodes (Fig. 5). The representative nature of the adult model geometry with the general population was ensured by comparing the model dimensions with the anatomical geometric data. The material properties for each component along with the literature source are summarized in Table 1.

The one-year-old finite element model included the vertebral centrum, bilateral neurocentral cartilages, rostral and caudal growth plates, bilateral costal cartilages of the transverse processes, posterior spinous processes cartilages, facet joints with more horizontal orientation, relatively larger nucleus pulposus of the intervertebral disc, and loosely embedded weak fibers in the ground substance. Figures 1, 2, and 3 illustrate these typical anatomical characteristics. The finite elements used for the individual spinal components and their material properties with the literature
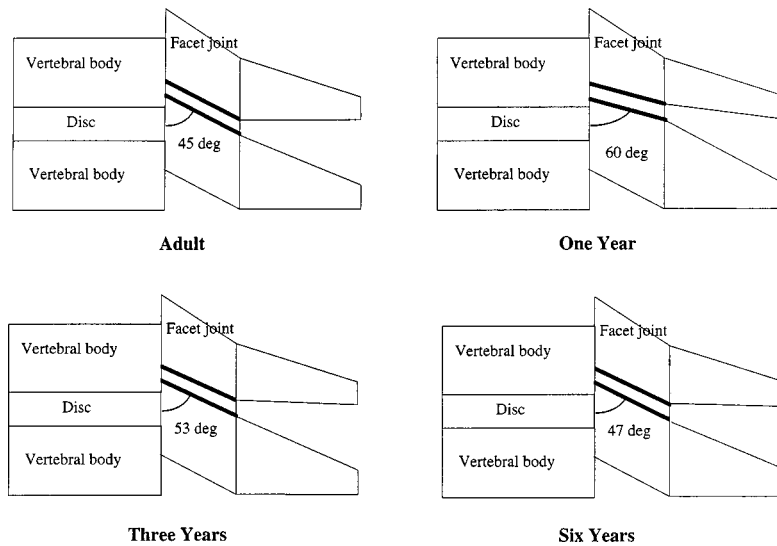
Fig. 2 Illustration of cervical spine facet joint orientation in the one-, three-, and six-year-old, and adult human cervical spine. In pediatric spines, the facet joint orientations are flatter. As age progresses, the facet joint becomes more inclined.

source are shown in Table 2. The three-year-old finite element model was constructed from the one-year-old model by incorporating fusion of the neural arches at the posterior spinous process–cartilage junction, tilting of the facet joint toward the transverse plane, and increase in volume and stiffness of the annulus fibers in the intervertebral discs (Figs. 1–3). Table 3 provides details of the finite elements and material properties of each spinal component used in the model with the literature source. The six-year-old model was developed from the three-year-old model by simulating the fusion of the vertebral centrum and neural arches at the neurocentral cartilages, fusion of neural arches at the costal cartilages of transverse processes, and increase in the volume of the annulus fibers with accentuated stiffness and decrease in the horizontal orientation of the facet joint anatomy (Figs. 1–3). Table 4 includes details of the finite elements and material properties of the spinal components used in the six-year-old cervical spine. The material property values and idealizations for each component in finite element models were adopted from literature [16–18,20–33]. I-DEAS and ABAQUS software were used to develop the
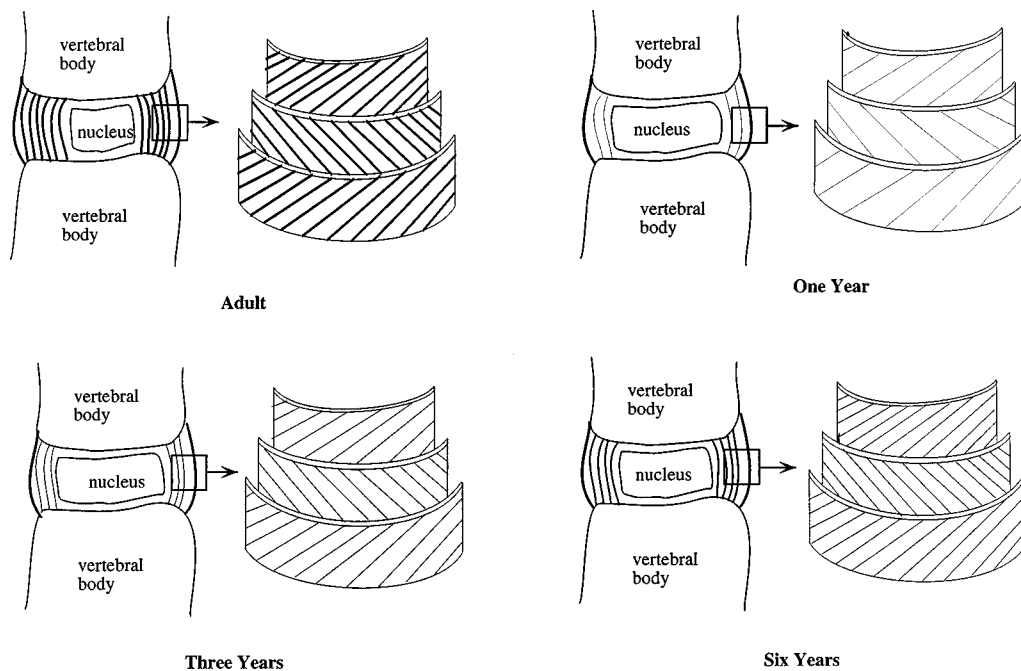
Fig. 3 Illustration of the intervertebral disc components in the one-, three-, and six-year-old, and adult human cervical spine. Left: sagittal section; right: magnified view of the annulus laminates showing the arrangement of fibers in the ground substance. The discs in pediatric spines are characterized by a relatively larger size nucleus with a lack of clear demarcation between the loosely embedded fibers in the ground substance and nucleus pulposus. As age advances, the fibers in the ground substance stiffen and distinguish the annulus from the nucleus.
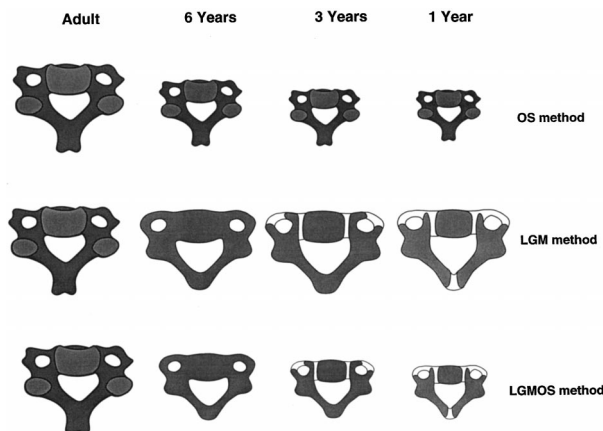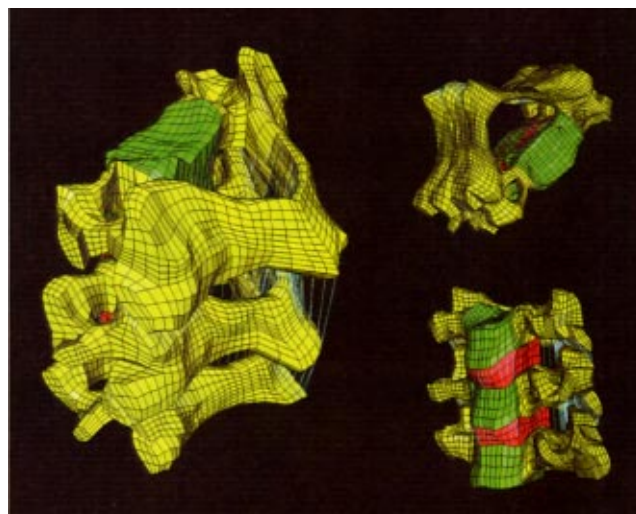
Fig. 4 Schematic representation demonstrating superior view of typical cervical vertebra. Illustration demonstrates the methodology used in the study. In OS method, the models were obtained from the adult model with simple scaling down to represent the pediatric models. In LGM method, the adult model was modified to incorporate age-specific local component material changes based upon the pediatric development process. This method did not include downward "size" scaling. In LGMOS approach, the modified adult models were scaled down to simulate the pediatric spine. In other words, this method applies the principles used in OS method to the models developed in LGM method.

Fig. 5 Different views of finite element mesh of ligamentous adult C4–C5–C6 spine. Left: Postero-lateral view. Top right: Superior view. Bottom right: Anterolateral view.

nonlinear finite element model of human cervical spine [34,35] ABAQUS software was used to conduct nonlinear analysis and post-processing.

All finite element models were exercised under pure compression (200 N), pure flexion and extension moments (0.5 Nm), and eccentric compression–flexion and compression–extension (200 N) loading modes. The inferior surface of the inferior-most vertebra was fixed in all degrees-of-freedom, and the external load was applied at the superior surface of the superior-most vertebra. The compression–flexion loads were applied at 1 cm ($A1$) and 2 cm ($A2$) anterior to the posterior longitudinal ligament. The compression–extension loads were applied at 1 cm ($P1$) and 2 cm ($P2$) posterior to the posterior longitudinal ligament. Pure compression was applied uniformly on the superior surface of the entire superior vertebra. Pure moments were applied as a force couple through the rigid plate attached to the superior vertebra. Eccentric loads were applied to the top surface of the rigid plate simulating knife-edge force application with reference to posterior longitudinal ligament. Under pure compression, the superior-most vertebra was unconstrained only in the superior–inferior direction under pure compression. Under moment loading, the degrees-of-freedom at the force-couple nodes in the plate were unconstrained in the direction of force. Under eccentric loads, the degrees-of-freedom at the knife-edge in the plate were unconstrained only in the direction of the application of the force. The same boundary and loading conditions were applied to all finite element models. The effects of geometric (large deformation) and material nonlinearities were included in the finite element analyses. The resulting overall peak deformation and rotation of the models under forces (compression and eccentric loads) and moments (flexion and extension) were used to calculate the flexibility in each model.

The following three approaches were adopted to compute and compare the biomechanical responses of the pediatric spines with the adult spine (Fig. 4). The first approach accounted for only the pure scaling off the adult model. This was termed Overall Scaling approach (OS). In this approach, overall geometry of the adult model was scaled to obtain the representative pediatric response based on pure geometric scaling. The scaling procedure consisted of enhancing the size of the adult model to 125, 150, and 175 percent of the original (100 percent) size, and using the principles of linear regression analysis to extrapolate to the one-, three-, and six-year-old spine responses. The chosen particular geometric differences among cervical spine finite element models were all based on anthropometric data [36]. Mere shrinking of the finite elements used in the adult model was not possible due to the already existing small or very fine mesh. Further remarks on this issue are provided in the Discussion section. The second approach was termed Local Geometric and Material changes method (LGM). This approach accounted for all specific spinal component modifications (e.g., growth plates and neural cartilages) to the adult spine model according to age-related anatomy. However, overall geometry of the adult model was maintained in each age group. The third approach was termed Local Geometric and Material changes combined with Overall Scaling (LGMOS). This approach combined the previous two approaches. In other words, scaling factors were included in the pediatric model responses obtained from the previous method. All pediatric responses were normalized with the adult model response under all loading modes using the following relation: $PR_{a,b} = ((P_{a,b} - A_a)/A_a)*100$; PR = normalized pediatric response; A = adult response; P = pediatric response; a = loading mode; b = three approaches (OS, LGM, LGMOS).

Results

The biomechanical responses obtained using the three approaches indicated that pediatric spines are always more flexible than adult spine under all loading modes. The responses were dependent on the age of the pediatric spine and type of loading mode.

In the OS approach, the percentage increases in flexibilities of the one-, three-, six-year pediatric spine models were calculated using both linear and nonlinear regression equations. The R^2 value and 95 percent confidence interval limits were used to select the best fit between percentage change in flexibility and model size. The nonlinear regression fit was better than linear regression under pure compression, compression–flexion ($A1$), compression–flexion ($A2$), compression–extension ($P1$), and compression–extension ($P2$) loading modes (all $R^2=1$) (Figs. 6–12). The linear regression fit was better than nonlinear regression fit under pure flexion ($R^2=0.991$) and extension ($R^2=0.993$) loading. The one-year spine was most flexible, followed by three- and six-year-old spine under each loading mode. In general, the increases in flexibilities of pediatric spines were rela-

Table 1 Adult finite element model details

Components	Element type	E (MPa)	γ	Reference
Cortex	solid	12000	0.3	(Clausen, 1996; Saito et al., 1991 [49]; Sharma et al., 1995; Shirazi-Adl et al., 1984; Yamada, 1970)
Cancellous core	solid	100	0.2	(Lindahl, 1975; Shirazi-Adl et al., 1984; Yamada, 1970)
Endplate	solid	600	0.3	(Saito et al., 1991)
Posterior elements	solid	3500	0.25	(Clausen, 1996; Sharma et al., 1995; Shirazi-Adl et al., 1984)
Disc annulus ground substance	solid	4.7	0.45	(Shirazi-Adl et al., 1984; Wu and Yao, 1976; Yamada, 1970)
Disc annulus fibers	rebar	500 (20%)	0.3	(Ghosh, 1988; Lavaste et al., 1992; Pooni et al., 1986; Shirazi-Adl et al., 1984; Ueno and Liu, 1987)
Disc nucleus pulposus	fluid	1666.7 *		(Ueno and Liu, 1987)
Facet articular cartilages	solid	10.4	0.4	(Kempson, 1979)
Facet synovial fluid	fluid	1666.7 *		(Goel et al., 1995; Ueno and Liu, 1987)
Facet synovial membrane	membrane	12.0	0.4	(Yamada, 1970)
Uncovertebral synovial fluid	fluid	1666.7 *		(Goel et al., 1995; Ueno and Liu, 1987)
Uncovertebral synovial membrane	membrane	12.0	0.4	(Yamada, 1970)
Ligaments	cable			(Pintar, 1986)

ALL		PLL		ISL		LF		CL	
def. (mm)	force (N)	def. (mm)	force (N)	def. (mm)	force (N)	def. (mm)	force (N)	def. (mm)	force (N)
1.4	35.5	1.0	29.0	1.3	16.9	1.9	45.9	1.8	53.6
2.7	64.9	2.0	51.4	2.7	24.4	3.7	82.4	3.9	87.9
4.1	89.7	3.0	71.3	4.0	29.5	5.6	119.6	5.8	109.4
5.4	108.6	4.0	85.8	5.4	32.9	7.5	133.7	7.7	125.8
6.8	119.6	5.0	94.7	6.7	34.9	9.4	147.2	9.7	134.8

E – Young's modulus (MPa), * - Bulk modulus (MPa), γ - Poisson's ratio, % - Percentage of fibers in annulus fibrosus, ALL – Anterior Longitudinal Ligament, PLL – Posterior Longitudinal Ligament, ISL – Interspinous Ligament, LF – Ligamentum Flavum and CL – Capsular Ligament.

Data from References [16–18, 20, 21, 24, 25, 27, 28, 30–33, 50].

tively smaller under flexion and extension compared to other loading modes. In pure loading cases, the increases in flexibilities of one-, three-, and six-year-old spines were the highest in compression and lowest in flexion. In eccentric loading cases, the increases in flexibilities of pediatric spines were the highest in compression–extension ($P1$) and lowest in compression–flexion ($A1$).

In the LGM approach, the percentage increases in flexibilities of the one-, three-, and six-year-old spines were considerably higher than increases in flexibilities determined using the OS approach (Figs. 13–19). The one-year-old spine was the most flexible, followed by the three-and six-year-old spines under extension, flexion, and compression–flexion ($A2$). In contrast, the three-year-old spine was the most flexible compared to six- and one-year-old spines under compression, compression–flexion ($A1$), and compression–extension ($P1$ and $P2$). In pure loading cases, the increases in flexibilities of one-, three-, and six-year-old spines were the highest in compression and lowest in flexion. In eccentric loading cases, the increases in flexibilities of pediatric spines were the highest in compression–extension ($P2$) and lowest in compression–extension ($P1$). While the flexibilities showed similar changes for the less eccentric compression–flexion ($A1$) and compression–extension ($P1$) loading cases, the percentage increases in the flexibilities were more pronounced for

the most eccentric compression–flexion ($A2$) and compression–extension ($P2$) loading cases. The response of the pediatric spine models in the LGMOS approach followed a similar pattern determined by using the LGM approach under all loading modes (Figs. 13–19). However, the percentage increases in flexibilities were higher compared to the LGM approach.

Discussion

To determine the biomechanical responses of the age-specific pediatric spine, it would be ideal to conduct experimental tests using pediatric cadaver spines. Unfortunately, pediatric tissues are not easily available for research. Consequently, as an alternative research tool, mathematical models such as finite element models can be used to obtain the biomechanical response of the pediatric spine. This technique has the unique ability to incorporate developmental anatomy features. In addition, it can simulate irregular and complex geometry, and heterogeneous material composition of cervical spine structures [13,18,20,27,31,37–45]. Furthermore, the technique allows for parametric studies. In this study, the finite element modeling technique was used to determine the biomechanical flexibility responses of the one-, three-, and six-year-old human pediatric cervical spines under various load combinations.

Table 2 One-year-old pediatric finite element model details (LGM approach)

Components	Element type	E (MPa)	γ	Reference
Vertebral centrum	solid	75	0.29	(Kumaresan et al., 1997c; Saito et al., 1991)
Cartilage plate	solid	25	0.4	(Melvin, 1995; Yamada, 1970)
Costal elements	solid	25	0.4	(Melvin, 1995; Yamada, 1970)
Posterior elements	solid	200	0.25	(Kumaresan et al., 1997c)
Posterior synchondrosis	solid	25	0.4	(Melvin, 1995; Yamada, 1970)
Neurocentral synchondrosis	solid	25	0.4	(Melvin, 1995; Yamada, 1970)
Disc annulus ground substance	solid	4.2	0.45	(Galante, 1967; Saito et al., 1991; Ueno and Liu, 1987; Wu and Yao, 1976)
Disc annulus fibers	rebar	400 (10%)	0.3	(Galante, 1967; Saito et al., 1991; Ueno and Liu, 1987; Wu and Yao, 1976)
Disc nucleus pulposus	fluid	1666.7 *		(Goel et al., 1995; Ueno and Liu, 1987)
Facet articular cartilages	solid	10.4	0.4	(Kempson, 1979)
Facet synovial fluid	fluid	1666.7 *		(Goel et al., 1995; Ueno and Liu, 1987)
Facet synovial membrane	membrane	12	0.4	(Yamada, 1970)
Ligaments	cable			(Pintar, 1986; Saito et al., 1991)

ALL		PLL		ISL		LF		CL	
def. (mm)	force (N)	def. (mm)	force (N)	def. (mm)	force (N)	def. (mm)	force (N)	def. (mm)	force (N)
1.4	28.4	1.0	23.2	1.3	13.5	1.9	36.7	1.8	42.9
2.7	51.9	2.0	41.1	2.7	19.5	3.7	65.9	3.9	70.3
4.1	71.8	3.0	57.0	4.0	23.6	5.6	95.7	5.8	87.5
5.4	86.9	4.0	68.6	5.4	26.3	7.5	106.9	7.7	100.6
6.8	95.7	5.0	75.8	6.7	27.9	9.4	117.8	9.7	107.8

E – Young's modulus (MPa), * - Bulk modulus (MPa), γ - Poisson's ratio, % - Percentage of fibers in annulus fibrosus, ALL – Anterior Longitudinal Ligament, PLL – Posterior Longitudinal Ligament, ISL – Interspinous Ligament, LF – Ligamentum Flavum and CL – Capsular Ligament.

Data from References [21, 22, 24, 25, 26, 29, 30, 32, 33, 39, 50].

The reasons for selecting the one-, three-, and six-year-old age groups were primarily based on characteristic anatomical changes, which are described in the Introduction section.

In the present study, three approaches were used to determine the flexibility characteristics of the pediatric spine for the following reasons. Because of a paucity of experimental data on pediatric structures, researchers have adopted an overall scaling approach. This method involves estimating pediatric responses using the principles of pure geometric similitude based on the adult structure. This procedure ignores component-specific anatomical changes. In effect, this procedure merely provides a scale factor to convert the adult model to the pediatric model. In the present study, this amounts to decreasing the size of the adult model by the age-related specific scale factor and exercising it under the seven loading conditions. In principle, it is possible to obtain a scaled-down version of the adult model to represent the specific age group pediatric model. However, this was not feasible because of the small size of the individual finite elements and the intricacy of spinal component details. For example, the facet joints were simulated by a fine mesh of synovial fluid encapsulated by the synovial membrane, capsular ligament, articular cartilage, and lateral masses. Initial efforts to exercise such reduced-size models were unsuccessful because numerical instabilities occurred. An indirect approach was therefore used. This was done by enhancing the adult model size (125, 150, and 175 percent), determining their flexibility responses, and extrapolating to a reduced size corresponding to each pediatric age group using linear and nonlinear regression equations (Figs. 6–12). Variations in individual age group flexibilities, although not considerably different, represent behavior of the pediatric spine as a function of loading mode, a set of results not previously reported in literature.

The effect of inclusion of the spinal component composition cannot be determined using the above-described pure geometric scaling approach. Consequently, the adult model was suitably modified to incorporate the necessary local component geometric and material properties changes (described earlier) representative of each pediatric group, i.e., LGM approach. However, this method did not account for the overall geometric size reduction for each age group. Using this approach, the adult, one-, three-, and six-year-old models were subjected to seven loading conditions. As in the pure geometric approach, all pediatric models were more flexible than the adult under all loading modes (Figs. 13–19). However, the pattern of increases in flexibilities did not follow the pattern found in the pure geometric approach. The

Table 3 Three-year-old pediatric finite element model details (LGM approach)

Components	Element type	E (MPa)	γ	Reference
Vertebral centrum	solid	75	0.29	(Kumaresan et al., 1997c; Saito et al., 1991)
Cartilage plate	solid	25	0.4	(Melvin, 1995; Yamada, 1970)
Costal elements	solid	25	0.4	(Melvin, 1995; Yamada, 1970)
Posterior elements	solid	200	0.25	(Kumaresan et al., 1997c)
Neurocentral synchondrosis	solid	25	0.4	(Melvin, 1995; Yamada, 1970)
Disc annulus ground substance	solid	4.2	0.45	(Galante, 1967; Saito et al., 1991; Ueno and Liu, 1987; Wu and Yao, 1976)
Disc annulus fibers	rebar	425 (15%)	0.3	(Galante, 1967; Saito et al., 1991; Ueno and Liu, 1987; Wu and Yao, 1976)
Disc nucleus pulposus	fluid	1666.7 *		(Goel et al., 1995; Ueno and Liu, 1987)
Facet articular cartilages	solid	10.4	0.4	(Kempson, 1979)
Facet synovial fluid	fluid	1666.7 *		(Goel et al., 1995; Ueno and Liu, 1987)
Facet synovial membrane	membrane	12	0.4	(Yamada, 1970)
Ligaments	cable			(Pintar, 1986; Saito et al., 1991)

ALL		PLL		ISL		LF		CL	
def. (mm)	force (N)	def. (mm)	force (N)	def. (mm)	force (N)	def. (mm)	force (N)	def. (mm)	force (N)
1.4	30.2	1.0	24.7	1.3	14.4	1.9	39.1	1.8	45.6
2.7	55.2	2.0	43.7	2.7	20.7	3.7	70.1	3.9	74.7
4.1	76.3	3.0	60.6	4.0	25.1	5.6	101.7	5.8	92.9
5.4	92.3	4.0	72.9	5.4	27.9	7.5	113.6	7.7	106.9
6.8	101.7	5.0	80.5	6.7	29.7	9.4	125.1	9.7	114.6

E – Young's modulus (MPa), * - Bulk modulus (MPa), γ - Poisson's ratio, % - Percentage of fibers in annulus fibrosus, ALL – Anterior Longitudinal Ligament, PLL – Posterior Longitudinal Ligament, ISL – Interspinous Ligament, LF – Ligamentum Flavum and CL – Capsular Ligament.

Data from References [21, 22, 24–26, 29, 30, 32, 33, 50].

considerably higher flexibility in the LGM approach compared to the OS approach stems from the relatively softer components of individual spines. In the third approach, the effect of both local component geometry and material changes, and overall scaling, were included by combining the two methodologies described above. An evaluation of these results indicates the influence of each approach on pediatric response.

In all approaches, pediatric responses were more flexible than the adult. Pure overall geometric scaling produced the least increase in flexibilities (Figs. 13–19). However, flexibility characteristics of the pediatric spine were profoundly affected by inclusion of the developmental anatomy of individual age group components (LGM approach). In contrast, the addition of the geometric size factor (LGMOS approach) further enhanced the variations in flexibilities; the increases were, however, not considerable compared to the LGM approach. The pattern of changes in flexibilities was uniform for the OS approach, i.e., maximum increase occurred for the one-year-old compared to the three- and six-year-old spines under all loading modes. However, such uniformly increasing tendencies were not apparent in the other two approaches, i.e., the responses of one-, three-, and six-year-old spines varied with type of loading mode. For example, the three-year-old spine was most flexible, followed by the six-and one-year-old spines under compression, compression–extension ($P1$ and $P2$), and compression–flexion ($A1$) loading. The more horizontal orientation of facet joint anatomy in the one-year-old spine may contribute to the additional resistance to flexibility under these loads. In addition, the local anatomical variations such as superior and inferior growth plates, bilateral neurocentral cartilages, and posterior spinous processes junction in the one-year spine also add to the structural response. When the age-specific pediatric spines were scaled (LGMOS approach), although the flexibility of the one-, three-, and six-year-old spines increased slightly, the pattern of flexibilities remained similar to the variation in flexibilities found in the LGM approach. These results indicate the overriding effect of local component geometric and material properties changes on biomechanical response of the pediatric spine.

Since the adult finite element model is representative of the mature human population, and since the three specific age groups were derived from the adult human, the three pediatric models developed in the present study are considered to be representative. Despite these similarities, it must be emphasized that the model includes only the C4, C5, and C6 vertebral units. For a full prediction of behavior of the entire column, the model needs to be extended to include the superior and inferior levels of the cervical spine. In addition, the current models account for the behavior of the pure ligamentous spine. Experimental studies are needed using

**Table 4 Six-year-old pediatric finite element model details (LGM approach)**

Components	Element type	E (MPa)	γ	Reference
Vertebral centrum	solid	75	0.29	(Kumaresan et al., 1997c; Saito et al., 1991)
Cartilage plate	solid	25	0.4	(Melvin, 1995; Yamada, 1970)
Posterior elements	solid	200	0.25	(Kumaresan et al., 1997c)
Disc annulus ground substance	solid	4.2	0.45	(Galante, 1967; Saito et al., 1991; Ueno and Liu, 1987; Wu and Yao, 1976)
Disc annulus fibers	rebar	450 (20%)	0.3	(Galante, 1967; Saito et al., 1991; Ueno and Liu, 1987; Wu and Yao, 1976)
Disc nucleus pulposus	fluid	1666.7 *		(Goel et al., 1995; Ueno and Liu, 1987)
Facet articular cartilages	solid	10.4	0.4	(Kempson, 1979)
Facet synovial fluid	fluid	1666.7 *		(Goel et al., 1995; Ueno and Liu, 1987)
Facet synovial membrane	membrane	12	0.4	(Yamada, 1970)
Ligaments	cable			(Pintar, 1986; Saito et al., 1991)

ALL		PLL		ISL		LF		CL	
def. (mm)	force (N)	def. (mm)	force (N)	def. (mm)	force (N)	def. (mm)	force (N)	def. (mm)	force (N)
1.4	31.9	1.0	26.1	1.3	15.2	1.9	41.3	1.8	48.2
2.7	58.4	2.0	46.3	2.7	21.9	3.7	74.2	3.9	79.1
4.1	80.7	3.0	64.2	4.0	26.6	5.6	107.6	5.8	98.5
5.4	97.7	4.0	77.2	5.4	29.6	7.5	120.3	7.7	113.2
6.8	107.6	5.0	85.2	6.7	31.4	9.4	132.5	9.7	121.3

E – Young's modulus (MPa), * - Bulk modulus (MPa), γ - Poisson's ratio, % - Percentage of fibers in annulus fibrosus, ALL – Anterior Longitudinal Ligament, PLL – Posterior Longitudinal Ligament, ISL – Interspinous Ligament, LF – Ligamentum Flavum and CL – Capsular Ligament.
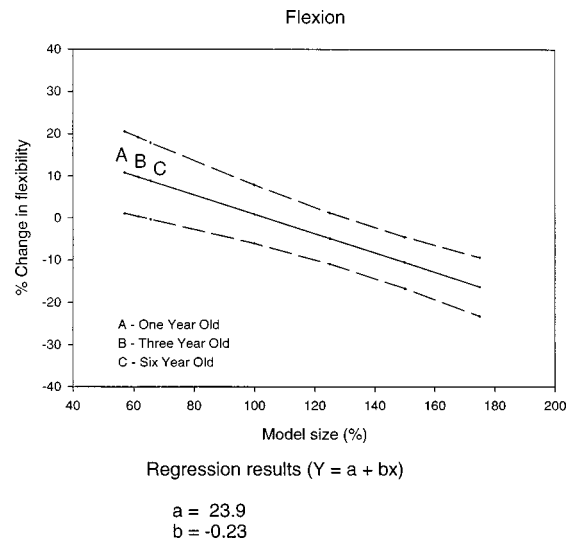
Data from References [21, 22, 24–26, 29, 30, 32, 33, 50].

Compression

Regression results (Y = a + b1x + b2x^2)

a = 85.426
b1 = -1.084
b2 = 2.296e-3
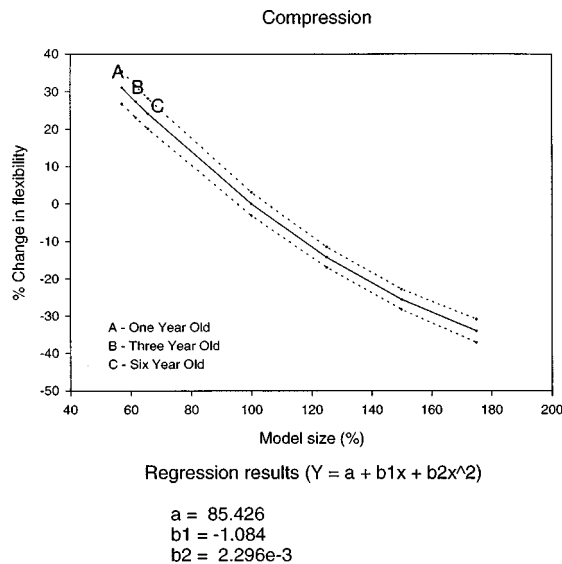
Fig. 6 Computation of one-, three-, and six-year-old pediatric spine responses by extrapolating the adult spine response under compression using nonlinear regression. The dotted lines represent 95 percent confidence limits.

Flexion

Regression results (Y = a + bx)

a = 23.9
b = -0.23

Fig. 7 Computation of one-, three-, and six-year-old pediatric spine responses by extrapolating the adult spine response under flexion using linear regression. The dotted lines represent 95 percent confidence limits.

the pediatric spines for additional conformation of the modeling output. Despite these limitations, and because of the paucity of data, the present results serve as a first step in the understanding of biomechanical behavior for this group of the human population.

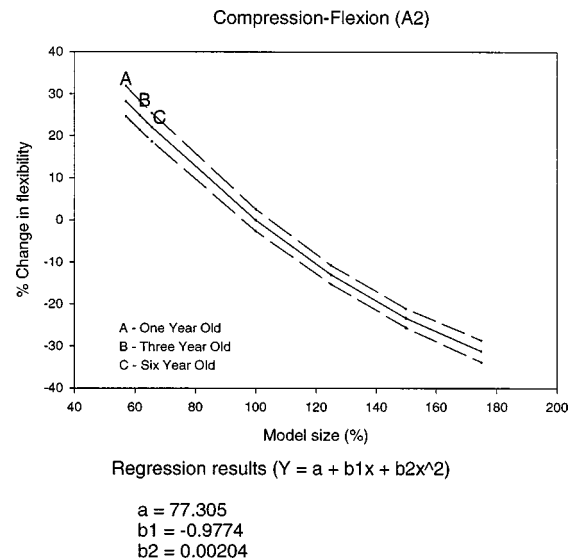It is well known that the spinal components do not follow the

principles of linear elasticity. Despite this knowledge, in the present study, the majority of spinal components was simulated as linear and isotropic materials. Ligaments were treated as nonlinear because of the availability of experimental data [30]. Synovial fluid in the uncovertebral and facet joints, and the nucleus pulposus in the intervertebral discs were simulated using incompress-

Extension

Regression results (Y = a + bx)

a = 27.664
b = -0.26732
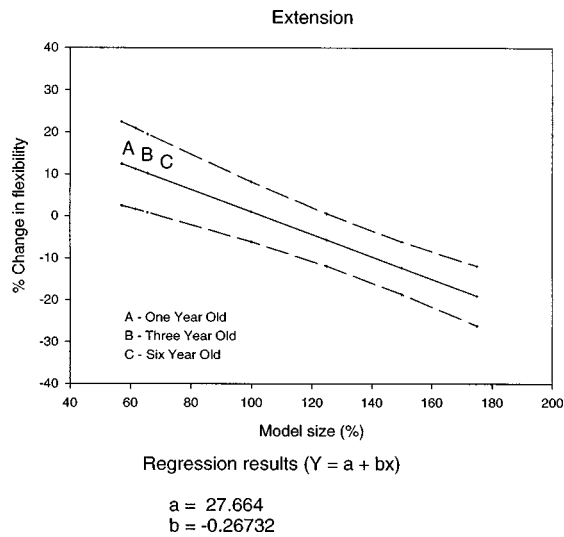
Fig. 8 Computation of one-, three-, and six-year-old pediatric spine responses by extrapolating the adult spine response under extension using linear regression. The dotted lines represent 95 percent confidence limits.

Compression-Flexion (A2)

Regression results (Y = a + b1x + b2x^2)

a = 77.305
b1 = -0.9774
b2 = 0.00204

Fig. 10 Computation of one-, three-, and six-year-old pediatric spine responses by extrapolating the adult spine response under compression−flexion ($A2$) using nonlinear regression. The dotted lines represent 95 percent confidence limits.

ible fluid elements because studies have indicated that these joints are incompressible [46,18]. The other components were treated as linear and elastic. They are the cortical shell, cancellous bone, posterior bony elements of the vertebra, and the annulus fibrosis of the disc. Because of the rigidity of the cortex (very high elastic modulus, $E = 12,000$ MPa), in spine biomechanics modeling, it is often treated as linear and elastic [24,47,31]. A similar argument has been advanced for the posterior elements of the vertebra [24,31]. Therefore, the present choice of material representation is in line with the previous studies. The annulus fibers of the disc have been modeled using nonlinear [31] and linear assumptions [24,21]. However, it has been reported that the nonlinear load-deformation behavior of the disc material is due to geometric nonlinearity of the annulus fibers embedded in ground substance rather than material nonlinearity [48]. Consequently, we used the linear properties for the annulus fibers of the intervertebral disc. It

should be noted that it is possible to include nonlinear definitions for these materials if and when the experimental data become available. Another justification is that even after three to five decades of lumbar spine research, finite element modelers with focus on multi-segments (like the one used herein) are still using linear properties [49]. This is because of the overriding influence, and we need to include fluid element representations and ligament nonlinearity before adding other component nonlinear material behavior. Nonetheless, the present model can be improved by incorporating nonlinearities for other materials; this points up an urgent need to obtain such experimental data from the human cervical spine.
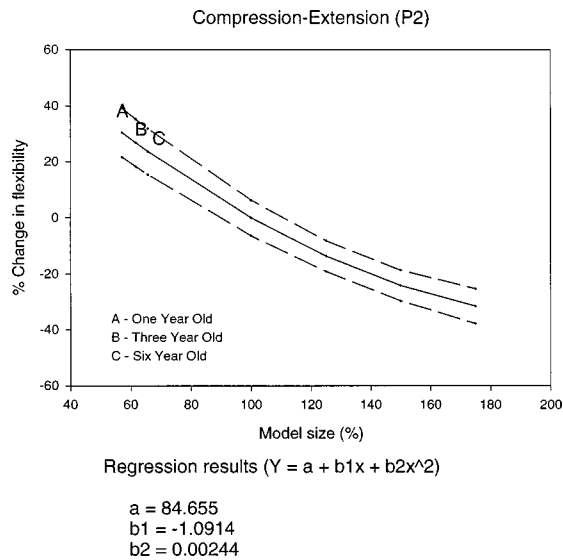
In summary, one-, three-, and six-year-old pediatric human cervical spine finite element models were developed by incorporating developmental anatomical features, and biomechanical responses
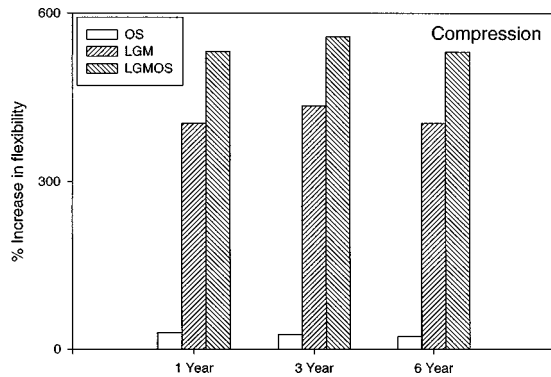
Compression-Flexion (A1)

Regression results (Y = a + b1x + b2x^2)

a = 68.305
b1 = -0.847
b2 = 0.0016
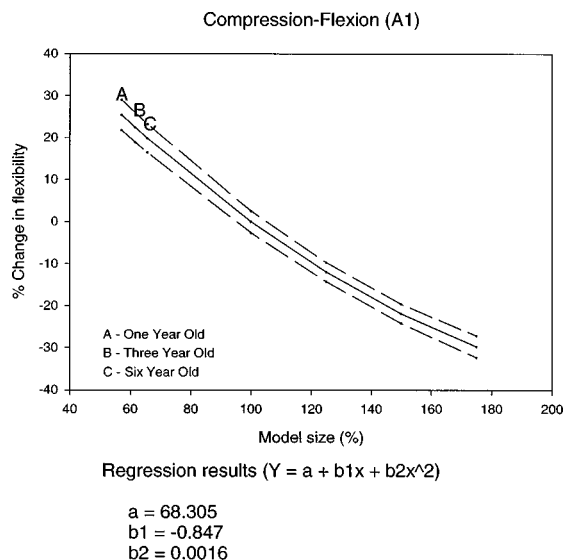
Fig. 9 Computation of one-, three-, and six-year-old pediatric spine responses by extrapolating the adult spine response under compression−flexion ($A1$) using nonlinear regression. The dotted lines represent 95 percent confidence limits.

Compression-Extension (P1)

Regression results (Y = a + b1x + b2x^2)

a = 83.335
b1 = -1.0618
b2 = 0.00228
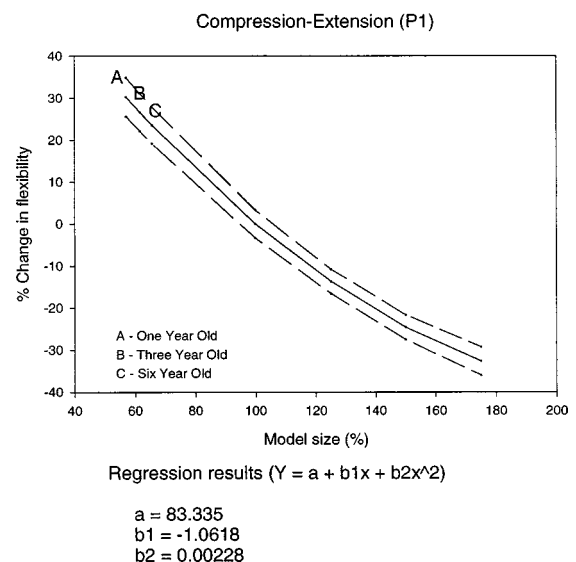
Fig. 11 Computation of one-, three-, and six-year-old pediatric spine responses by extrapolating the adult spine response under compression−extension ($P1$) using nonlinear regression. The dotted lines represent 95 percent confidence limits.

Fig. 12 Computation of one-, three-, and six-year-old pediatric spine responses by extrapolating the adult spine response under compression−extension ($P2$) using nonlinear regression. The dotted lines represent 95 percent confidence limits.
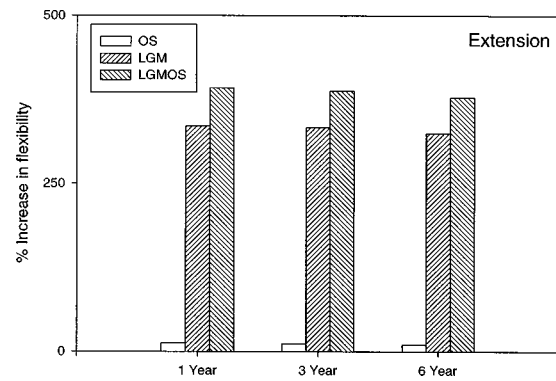

Fig. 13 Percentage increase in flexibilities in one-, three-, and six-year-old spine responses computed using OS, LGM, and LGMOS approaches under compression
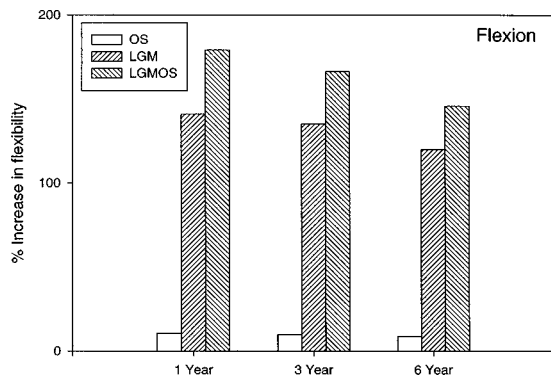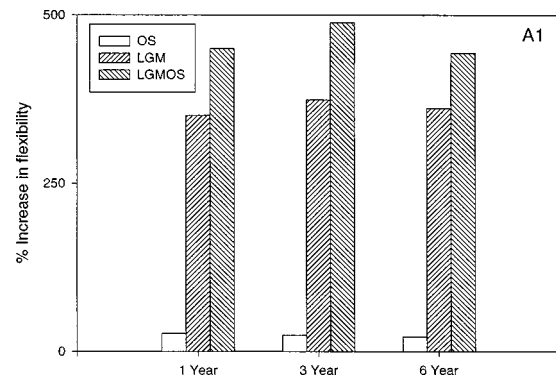

Fig. 14 Percentage increase in flexibilities in one-, three-, and six-year-old spine responses computed using OS, LGM, and LGMOS approaches under flexion

Fig. 15 Percentage increase in flexibilities in one-, three-, and six-year-old spine responses computed using OS, LGM, and LGMOS approaches under extension

Fig. 16 Percentage increase in flexibilities in one-, three-, and six-year-old spine responses computed using OS, LGM, and LGMOS approaches under compression−flexion ($A1$)

Fig. 17 Percentage increase in flexibilities in one-, three-, and six-year-old spine responses computed using OS, LGM, and LGMOS approaches under compression−flexion ($A2$)
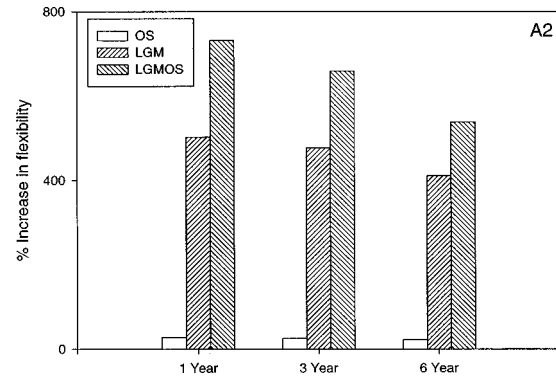
were computed and compared with that of the adult spine under various loading conditions. Effects of pure overall geometric scaling from the adult spine, local component developmental anatomy variations that occur to the age-specific pediatric spines, and geometric scaling combined with local component anatomy variations were studied. The pediatric spine responses obtained with pure overall (only geometric) scaling of the adult spine indicated that flexibilities consistently increased in a uniform manner from the six- to one-year-old spine under all loading cases. In contrast, incorporation of local anatomic changes specific to pediatric spines in the three age groups (maintaining the same adult size) resulted not only in a considerable increase in flexibility, but responses also varied as a function of age of the pediatric spine and type of external loading. When the geometric scaling effects were added to the above-mentioned actual pediatric spines, increases in flexibility were slightly higher; however, the pattern of responses
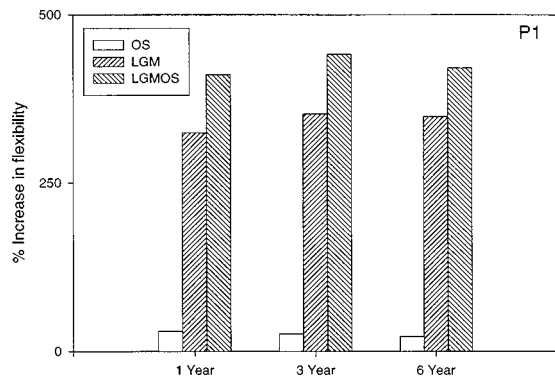
Fig. 18   Percentage increase in flexibilities in one-, three-, and six-year-old spine responses computed using OS, LGM, and LGMOS approaches under compression−extension (P1)
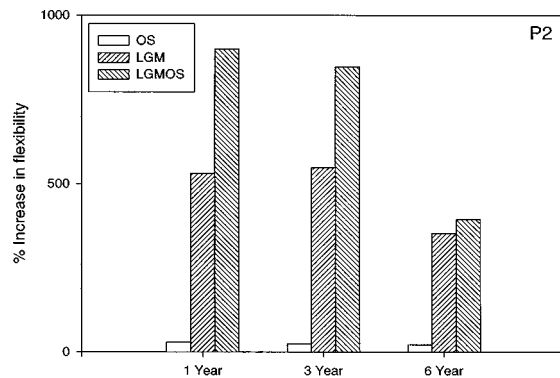
Fig. 19   Percentage increase in flexibilities in one-, three-, and six-year-old spine responses computed using OS, LGM, and LGMOS approaches under compression−extension (P2)

remained the same as those found in the previous approach. These results indicate that inclusion of developmental anatomical changes characteristic of the pediatric spines has more of an effect on biomechanical responses than extrapolating responses of the adult spine based on pure overall geometric scaling.

References

[1] Burdi, A. R., Huelke, D. F., Snyder, R. G., and Lowrey, G. H., 1969, ''Infants and Children in the Adult World of Automobile Safety Design: Pediatric and Anatomical Considerations for Design of Child Restraints,'' J. Biomech., **2**, pp. 267–280.

[2] Hayashi, K., and Yabuki, T., 1985, ''Origin of the Uncus and of Luschka's Joint in the Cervical Spine,'' J. Bone Joint Surg., **67A**, pp. 788–791.

[3] Hindman, B., and Poole, C., 1970, ''Early Appearance of the Secondary Vertebral Ossification Centers,'' Radiology, **95**, pp. 359–361.

[4] Knutsson, F., 1961, ''Growth and Differentiation of Postnatal Vertebra,'' Acta Radiol., **55**, pp. 401–408.

[5] Roaf, R., 1960, ''Vertebral Growth and Its Mechanical Control,'' J. Bone Joint Surg., **42B**, pp. 40–59.

[6] O'Rahilly, R., and Benson, D., 1985, ''Development of Vertebral Column,'' in: The Pediatric Spine, D. Bradford and R. Hensinger, eds., Thieme, Inc., New York, pp. 3–17.

[7] Sherk, H. H., Dunn, E. J., Eismont, F. J., Fielding, J. W., Long, D. M., Ono, K., Penning, L., and Raynor, R., 1989, The Cervical Spine, J. B. Lippincott Co., Philadelphia, PA.

[8] Peacock, A., 1956, ''Observations on Postnatal Structure of Intervertebral Disc in Man,'' J. Anat., **86**, pp. 162–179.

[9] Taylor, J., 1975, ''Growth of Human Intervertebral Discs and Vertebral Bodies,'' J. Anat., **120**, pp. 49–68.

[10] Kasai, T., Ikata, T., Katoh, S., Miyake, R., and Tsubo, M., 1996, ''Growth of Cervical Spine With Special Reference to Its Lordosis and Mobility,'' Spine, **21**, pp. 2067–2073.

[11] Bailey, D., 1952, ''Normal Cervical Spine in Infants and Children,'' Radiology, **59**, pp. 712–719.

[12] Kumaresan, S., Yoganandan, N., Pintar, F., Voo, L., Cusick, J., and Larson, S., 1997, ''Finite Element Modeling of Cervical Laminectomy With Graded Facetectomy,'' J. Spinal Disord., **10**, pp. 40–47.

[13] Kumaresan, S., Yoganandan, N., and Pintar, F. A., 1998, ''Finite Element Modeling Approaches of Human Cervical Spine Facet Joint Capsule,'' J. Biomech., **31**, pp. 371–376.

[14] Kumaresan, S., Yoganandan, N., and Pintar, F. A., 1999, ''Finite Element Analysis of the Cervical Spine: A Material Property Sensitivity Study,'' Clinical Biomechanics, **14**, pp. 41–53.

[15] Yoganandan, N., Kumaresan, S., Voo, L., and Pintar, F., 1997, ''Finite Element Model of the Human Lower Cervical Spine,'' ASME J. Biomech. Eng., **119**, pp. 87–92.

[16] Gosh, P., 1988, Biology of the Intervertebral Disc, CRC Press, Inc., Boca Raton, FL.

[17] Pooni, J. S., Hukins, D. W., Harris, P. F., Hilton, R. C., and Davies, K. E., 1986, ''Comparison of the Structure of Human Intervertebral Discs in the Cervical, Thoracic and Lumbar Regions of the Spine,'' Surg. Radiol Anat., **8**, pp. 175–182.

[18] Shirazi-Adl, S. A., Shrivastava, S. C., and Ahmed, A. M., 1984, ''Stress Analysis of the Lumbar Disc-Body Unit in Compression: A Three-Dimensional Nonlinear Finite Element Study,'' Spine, **9**, pp. 120–134.

[19] Spilker, R., Jacobs, D., and Schultz, A., 1986, ''Material Constants for a Finite Element Model of the Intervertebral Disk With a Fiber Composite Annulus,'' ASME J. Biomech. Eng., **108**, pp. 1–11.

[20] Clausen, J. D., 1996, ''Experimental and Theoretical Investigation of Cervical Spine Biomechanics: Effects of Injury and Stabilization,'' Ph.D. thesis, University of Iowa, Iowa City.

[21] Ueno, K., and Liu, Y. K., 1987, ''A Three Dimensional Nonlinear Finite Element Model of Lumbar Intervertebral Joint in Torsion,'' ASME J. Biomech. Eng., **109**, pp. 200–209.

[22] Galante, J. O., 1967, ''Tensile Properties of the Human Lumbar Annulus Fibrosus,'' Acta Orthop. Scand. Suppl., **100**, p. 1–91.

[23] Goel, V. K., and Clausen, J. D., 1998, ''Prediction of Load Sharing Among Spinal Components of a C5–C6 Motion Segment Using the Finite Element Approach,'' Spine, **23**, pp. 684–691.

[24] Goel, V. K., Monroe, B. T., Gilbertson, L. G., and Brinckmann, P., 1995, ''Interlaminar Shear Stresses and Laminae Separation in a Disc: Finite Element Analysis of the L3–4 Motion Segment Subjected to Axial Compressive Loads,'' Spine, **20**, pp. 689–698.

[25] Kempson, G. E., 1979, ''Mechanical Properties of Articular Cartilage.'' in: Adult Articular Cartilage, Pitman, Kent, England, pp. 333–414.

[26] Kumaresan, S., Yoganandan, N., and Pintar, F. A., 1997, ''Adult and Pediatric Human Cervical Spine Finite Element Analyses,'' ASME BED, **35**, pp. 515–516.

[27] Lavaste, F., Skalli, W., Robin, S., Roy-Camille, R., and Mazel, C., 1992, ''Three Dimensional Geometrical and Mechanical Modeling of the Lumbar Spine,'' J. Biomech., **25**, pp. 1153–1164.

[28] Lindahl, D., 1975, ''Mechanical Properties of Dried Spongy Bone,'' Acta Orthop. Scand., **47**, pp. 11–19.

[29] Melvin, J. W., 1995, ''Injury Assessment Reference Values for the CRABI 6-Month Infant Dummy in a Rear-Facing Infant Restraint With Airbag Deployment,'' Proc. SAE Congress and Exposition, pp. 1–12.

[30] Pintar, F. A., 1986, ''Biomechanics of Spinal Elements,'' Doctoral Dissertation, Marquette University, Milwaukee, WI.

[31] Sharma, M., Langrana, N. A., and Rodriguez, J., 1995, ''Role of Ligaments and Facets in Lumbar Spinal Stability,'' Spine, **20**, pp. 887–900.

[32] Wu, H. C., and Yao, R. F., 1976, ''Mechanical Behavior of the Human Anulus Fibrosus,'' J. Biomech., **9**, pp. 1–7.

[33] Yamada, H., 1970, Strength of Biological Materials, Williams & Wilkins, Baltimore, MD.

[34] ABAQUS, 1994, ''ABAQUS—Standard User's Manual,'' Hibbitt, Karlsson & Sorensen, Inc.

[35] I-DEAS, 1994, ''I-DEAS MS,'' Structural Dynamics Research Corporation, Milford, OH.

[36] Snyder. R. G., 1977, ''Anthropometry of Infants, Children, and Youths to Age 18 for Product Safety Design,'' University of Michigan.

[37] Kleinberger, M., 1993, ''Application of Finite Element Techniques to the Study of Cervical Spine Mechanics,'' Proc. 37th Stapp Car Crash Conference, pp. 261–272.

[38] Kumaresan, S., Yoganandan, N., and Pintar, F., 1997, ''Finite Element Analysis of Anterior Cervical Spine Interbody Fusion,'' Biomed. Mat. & Eng., **7**, pp. 221–230.

[39] Kumaresan, S., Yoganandan, N., and Pintar, F. A., 1997, ''Pediatric Neck Modeling Using Finite Element Analysis,'' Inter. J. Crashworthiness, **2**, pp. 367–377.

[40] Langrana, N. A., Lee, C. K., and Yang, S. W., 1991, ''Finite Element Modeling of the Synthetic Intervertebral Disc,'' Spine, **16**, pp. 245–S252.

[41] Martinez, M., Anderson, R., Hart, R., Bundy, K., Dinh, D., Hew, M., and Aydin, F., 1997, ''Titanium Release From T1-6AL-4V Cervical Spine Plates:

A Computational and Experimental Study in the Canine Model,'' *Proc. 43rd Orthopaedic Research Society*, p. 215–236.

[42] Maurel, N., Lavaste, F., and Skalli, W., 1997, ''A Three Dimensional Parameterized Finite Element Model of the Lower Cervical Spine. Study of the Influence of the Posterior Articular Facets,'' J. Biomech., **30**, pp. 921–931.

[43] Yoganandan, N., Kumaresan, S., Voo, L., and Pintar, F., 1996, ''Finite Element Applications in Human Cervical Spine Modeling,'' Spine, **21**, pp. 1824–1834.

[44] Yoganandan, N., Myklebust, J. B., Ray, G., and Sances, A., Jr., 1987, ''Mathematical and Finite Element Analysis of Spinal Injuries,'' Crit. Rev. Biomed. Eng., **15**, pp. 29–93.

[45] Yoganandan, N., Pintar, F. A., Larson, S. J., Sances, A., Jr., eds., 1998, *Frontiers in Head and Neck Trauma: Clinical and Biomechanical*, IOS Press, Amsterdam, Netherlands.

[46] Kumaresan, S., Yoganandan, N., and Pintar, F. A., 1997, ''Methodology to Quantify the Uncovertebral Joint in the Human Cervical Spine,'' J. Musculoskeletal Research, **1**, pp. 131–139.

[47] Natarajan, R. N., Ke, J. H., and Andersson, B. J., 1994, ''A Model to Study the Disc Degeneration Process,'' Spine, **19**, pp. 259–265.

[48] Ueno, K., 1984, ''A Three Dimensional Nonlinear Finite Element Model of Lumbar Intervertebral Joint,'' University of Iowa.

[49] Goel, V. K., Kim, Y. E., Lim, T. H., and Weinstein, J. N., 1988, ''An Analytical Investigation of the Mechanics of Spinal Instrumentation,'' Spine, **13**, pp. 1003–1011.

[50] Saito, T., Yamamuro, T., Shikata, J., Oka, M., and Tsutsumi, S., 1991, ''Analysis and Prevention of Spinal Column Deformity Following Cervical Laminectomy. I. Pathogenetic Analysis of Postlaminectomy Deformities,'' Spine, **16**, pp. 494–502.